# Relaxation Processes in Poly(2-chlorocyclohexyl acrylate) As Studied by Dielectric Relaxation and Mechanical Relaxation Spectroscopy

**Ricardo Díaz-Calleja,[†] Evaristo Riande,*[,‡] Julio San Román,[‡] and Vicente Compañ[§]**

*Departamento de Termodinámica Aplicada, UPV, Valencia, Spain, Instituto de Polímeros, CSIC, 28006 Madrid, Spain, and Departamento de Ciencias Experimentales, Universidad Jaume I, Castellón, Spain*

*Received March 10, 1994; Revised Manuscript Received June 6, 1994*[⊗]

ABSTRACT: A comparative study of the mechanical and dielectric relaxation spectra of poly(2-chlorocyclohexyl acrylate) (PCCHA) is reported. The spectra present a moderate subglass $\beta$ absorption, followed in increasing temperature order by a prominent $\alpha$ glass–rubber relaxation process. The distribution of activation free energies for the $\beta$ subglass relaxation is determined, from which average values of 14.0 kcal mol$^{-1}$/6.94 cal mol$^{-1}$ K$^{-1}$ and 10.5 kcal mol$^{-1}$/1.83 cal mol$^{-1}$ K$^{-1}$ are obtained for activation enthalpies/entropies of the mechanical and dielectric processes, respectively. The critical analysis of the $^1$H NMR spectra and the modeling of the dielectric relaxation suggest that this absorption is mainly caused by conformational transitions about the C–CO bonds of the side groups. The fact that the exponent of the stretch function is similar for the $\alpha$ and $\beta$ relaxations seems to indicate that very limited local processes produce the $\beta$ absorption.

## Introduction

The mechanical behavior exhibited in the glassy state by polymers with flexible side groups is governed by molecular motions either taking place on the side groups alone or coupled with local motions of the main chain.[1–4] The considerable subglass mechanical activity found in polymers with cyclohexyl groups on the side chains has been attributed to chair-to-chair conformational transitions in the cyclohexyl ring because the activation energy associated with the mechanical relaxation, ca. 11 kcal mol$^{-1}$, nearly coincides with the barrier energy of that transition.[5]

The viscoelastic response of aliphatic polyesters with 1,4-cyclohexylene groups located in the backbone of the glycol residue is strongly dependent on the hydrogen substitutions equatorial/equatorial (trans isomers) or equatorial/axial (cis isomers) on the cyclohexane ring.[6] Whereas the cis isomers exhibit an ostensible mechanical $\beta$ relaxation located at −60 °C at 1 Hz, the relaxation spectrum of the trans isomer presents a broad subglass $\beta$ absorption that can be resolved in two overlapping peaks centered at −80 ($\beta_1$) and −105 °C ($\beta_2$). The mechanical response of polyformals in the glassy state, specifically poly(*cis*/*trans*-1,4-cyclohexanedimethanol-*alt*-formaldehyde),[7] seems to be similar to that exhibited by its polyester counterpart. The critical interpretation of the relaxation spectra of these polyesters and polyformals suggests that, whereas the $\beta$ absorption in the cis isomers is caused by conformational changes about the adjacent bonds to the cyclohexane ring in glycol residue, this relaxation in the trans isomers is presumably caused by molecular motions in which conformational changes involving skeletal bonds beyond those of the glycol residue take part. In any case, flipping of conformational transitions through the cyclohexane ring does not seem to play an important role in the mechanical behavior of these polymers in the glassy state.[6,7]

This work focuses on the study of the relaxation behavior of poly(2-chlorocyclohexyl acrylate) (PCCHA), with the aim of investigating how the presence of the halogen atom affects the mechanical response of the polymer in both the glassy state and the glass–rubber relaxation processes. Earlier studies carried out on poly(chlorocyclohexyl methacrylates) showed an important dielectric activity in the glassy state which was attributed to conformational chair-to-chair transitions which would move the halogen atom from equatorial to axial positions.[8] Therefore, the dielectric behavior of PCCHA is also investigated in parallel with the mechanical studies in order to obtain information relative to the origin of the mechanical and dielectric activity in the glassy state.

## Experimental Part

2-Chlorocyclohexyl acrylate was obtained by dropwise addition of freshly distilled acryloyl chloride to a cooled aqueous dioxane (20% dioxane) solution of 2-chlorocyclohexanol containing 5% NaOH. Crude 2-chlorocyclohexyl acrylate was extracted 2-fold with ether, washed with water, dried successively with calcium chloride and calcium hydride, and further distilled at reduced pressure.

Poly(2-chlorocyclohexyl acrylate) was prepared at 60 °C by radical polymerization of the monomer in benzene using AIBN as the initiator. The polymer was precipitated with methanol, dissolved in benzene, and precipitated again with methanol. Finally the polymer was dried at 60 °C in a high-vacuum line. The glass transition temperature of the polymer, determined with a Perkin-Elmer DSC calorimeter at the onset of the endotherm, was found to be 59 °C.

The real $\epsilon'$ and loss $\epsilon''$ components of the complex dielectric permittivity $\epsilon^*$ for PCCHA were determined as a function of both temperature and frequency with a three-terminal plane condenser and a capacitance apparatus TA DEA 2970 operating in the frequency range $10^{-1}$–$3 \times 10^4$ Hz. The real $E'$ and loss $E''$ components of the complex relaxation modulus $E^*$ were measured at five frequencies with a PL-DMTA Mark II apparatus in double-cantilever flexion. For both the mechanical and dielectric measurements, the experiments proceeded from low to high temperature at a heating rate of 1 °C/min.

[†] UPV.
[‡] CSIC.
[§] Universidad Jaume I.
[⊗] Abstract published in *Advance ACS Abstracts,* December 15, 1994.

0024-9297/95/2228-0614$09.00/0 

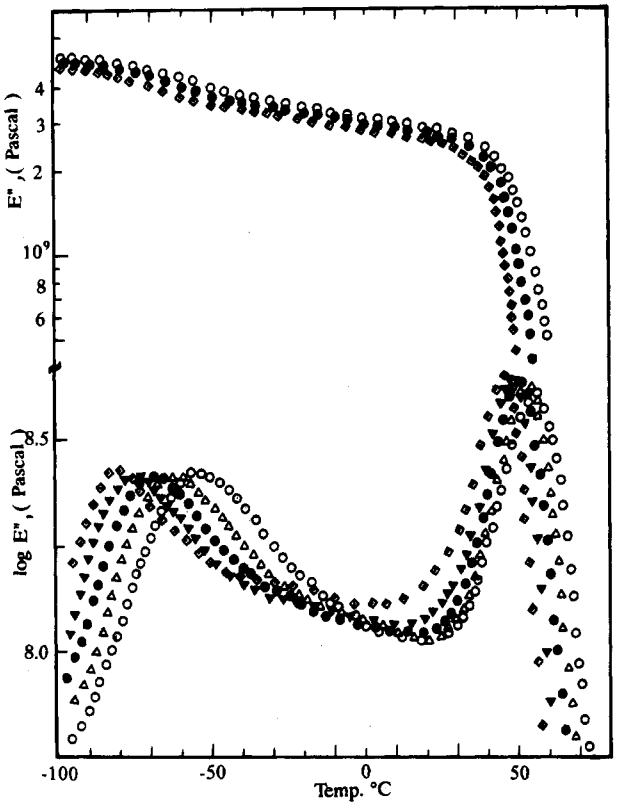


**Figure 1.** Temperature dependence of the storage ($E'$) and loss ($E''$) relaxation moduli at several frequencies: (◇) 0.1, (▼) 0.3, (●), 1, (△) 3, and (○) 10 Hz.

## Mechanical and Dielectric Results

The storage and loss relaxation moduli are represented as a function of temperature, at several frequencies, in Figure 1. The loss curves exhibit a moderate subglass absorption centered at −76 °C at 0.1 Hz ($\beta$ process), followed by a prominent glass−rubber relaxation ($\alpha$ process) centered at 62 °C at the same frequency. The $\beta$ relaxation is accompanied by a relatively small drop in the storage relaxation modulus, as a consequence of the moderate mechanical activity developed in the process. The dielectric spectrum, expressed in terms of the dielectric loss in Figure 2, also presents a subglass $\beta$ relaxation whose location is slightly shifted to the lower temperature side of the spectrum with respect to that of the mechanical $\beta$ absorption; the relaxation is followed in increasing temperature order by the glass−rubber relaxation, which at low frequencies is dominated by conductive processes. The separation of the conductive and dipolar relaxations can be achieved by writing the dielectric results in terms of the complex electric modulus $M^* = (\epsilon^*)^{-1}$. Actually, the complex dielectric plot, represented in Figure 3, shows three arcs which from left to right correspond to the conductive process, the dipolar glass−rubber relaxation, and the subglass $\beta$ process, respectively.

The mechanical and dielectric $\beta$ relaxations follow Arrhenius behavior, and the activation energies associated with these processes are 14 and 10 kcal mol$^{-1}$, respectively. In the determination of the activation energies only the maximum of either the isochrone or isotherm loss curves is considered without taking into account the remainder of the curves. The evaluation of the distribution of activation energies associated with the mechanisms intervening in the $\beta$ process requires the knowledge of the relaxation behavior over a wide range of frequencies.[9] However, the mechanical results

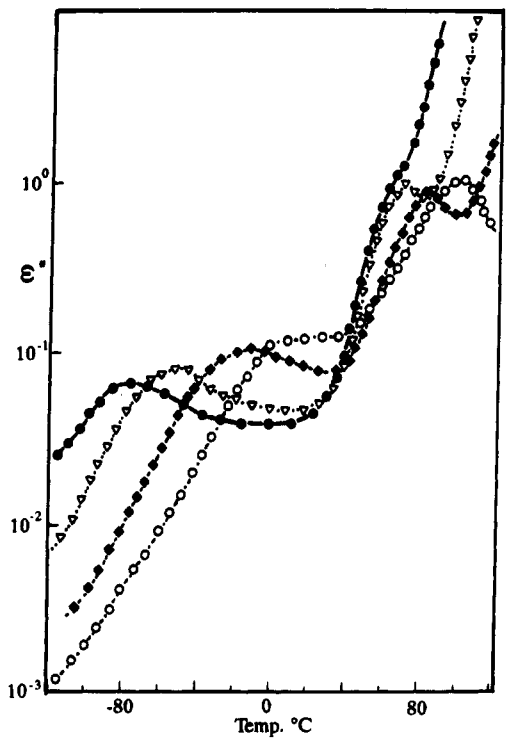


**Figure 2.** Variation of the dielectric loss $\epsilon''$ with temperature at several frequencies: (●) 1, (▽) 20, (◆) 500 and (○).

were performed over a very limited range of frequencies, and, consequently, the distribution of activation free energies could not be calculated with the available results. For that purpose, the mechanical and the dielectric subglass relaxations were adjusted to the semiempirical Fuoss−Kirkwood relation[10]

$$\Gamma''(\omega) = \Gamma''_{max}(\omega)\ \text{sech}\ m \ln(\omega/\omega_{max}) \qquad (1)$$

where $\Gamma''$ represents the mechanical/dielectric loss and $\Gamma''_{max}$ is the value of these quantities at the peak maximum; $m$ is a form parameter ($0 \le m \le 1$) that is related to the width of the relaxation in the sense that the larger $m$ is, the wider the distribution is, and $\omega$ is the angular frequency. The values of $\ln(\omega/\omega_{max})$ are related to the temperature by means of the expression

$$\ln \frac{\omega}{\omega_{max}} = \frac{E_a}{R}\left(\frac{1}{T} - \frac{1}{T_{max}}\right) \qquad (2)$$

The values of $m$ were directly determined from $\cosh^{-1}(\Gamma''_{max}/\Gamma'')$ *vs* $1/T$ plots, and the results obtained for the mechanical and dielectric $\beta$ relaxations are given in Table 1. As can be seen in Figure 4, the experimental mechanical loss curves fit very well to eq 1 in the high-frequency region; however, in the low-frequency zone, the experimental results depart from those predicted by the Fuoss−Kirkwood expression due to the overlapping of the $\beta$ relaxation process and the glass−rubber relaxation. The same behavior is exhibited by the $\beta$ dielectric relaxation process indicated in Figure 5. The relaxation strength of the mechanical and dielectric $\beta$ relaxation was then calculated from the relationship[11]

$$\Delta\Gamma = 2\Gamma''_{max}/m \qquad (3)$$

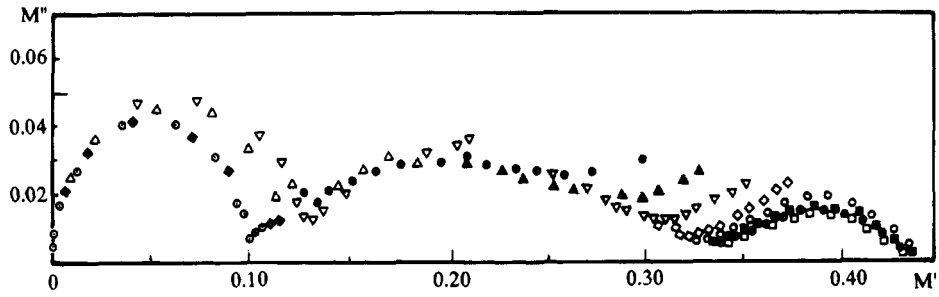


**Figure 3.** Complex dielectric plots for the dielectric modulus at several temperatures: (⊙) 119, (◆) 110, (△) 99.5, (▽) 90, (●) 69, (▲) 59, (▼) 30, (◇) 40, (○) 29.5, (■) 0, (⊖) −20 and (□) −40 °C.

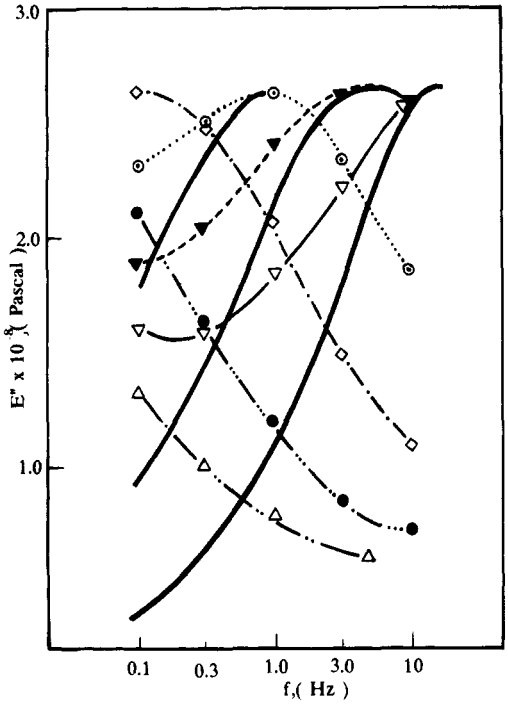


**Figure 4.** Frequency dependence of the loss relaxation modulus at several temperatures: (▽) −50, (▼) −60, (⊙) −70, (◇) −80, (●) −90, and (△) 136 °C. Continuous lines calculated using the Fuoss−Kirkwood equation.

**Table 1. Values of the Parameter $m$ in Equation 1 and Strengths of the Mechanical and Dielectric $\beta$ Relaxations at Different Temperatures**

| $T$, °C | $m$(mech.) | m(diel.) | $\Delta E_\beta$, × $10^9$ Pa | $\Delta\epsilon_\beta$ |
|---|---|---|---|---|
| −90 | 0.293 | | 1.77 | |
| −80 | 0.374 | | 1.40 | |
| −70 | 0.406 | 0.424 | 1.30 | 0.330 |
| −60 | | 0.448 | | 0.342 |
| −50 | | 0.472 | | 0.365 |
| −40 | | 0.496 | | 0.367 |
| −30 | | 0.521 | | 0.382 |

where $\Delta\Gamma$ represents $E_u - E_r$ and $\epsilon_r - \epsilon_u$ for the mechanical and dielectric relaxations, respectively, the subindices u and r referring to the relaxing and unrelaxing values of both the permittivity and the modulus.

The distribution of activation free energies $\Delta G^{**}$ associated with the mechanisms intervening in the $\beta$ relaxation was then obtained by using the absolute reaction rate theory to interpret the potential barrier that governs the process. According to the theory, $\Delta G^{**}$ is related to the angular frequency by the relation

$$\Delta G^{**} = RT\left(\ln\frac{\kappa}{h} + \ln\frac{T}{\omega}\right) \tag{4}$$

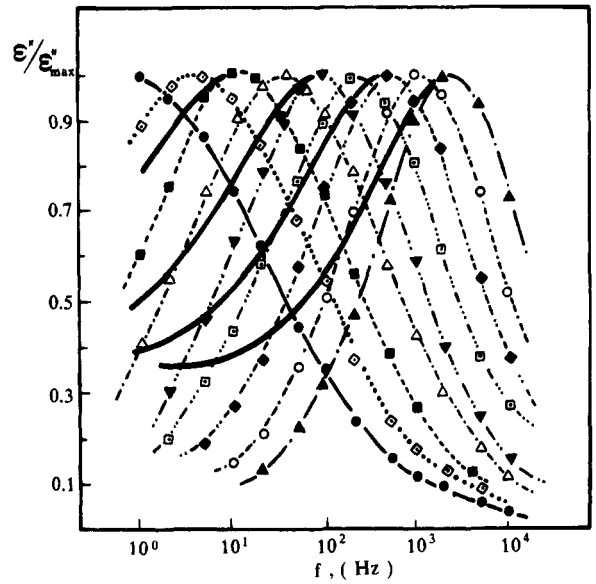


**Figure 5.** Curves calculated using the Fuoss−Kirkwood equation showing the frequency dependence of the normalized loss dielectric permittivity in the $\beta$ region at several temperatures: (▲) 0, (○) −10, (◆) −20, (⊡) −30, (▼) −40, (△) −50, (■) −60, (◇) −70, and (●) −80 °C. Continuous lines represent curves fitting the experimental results.

This equation in conjunction with the approximate expression for the relaxation spectrum[12,13]

$$\phi \approx \frac{2}{\pi}\frac{\Gamma''}{\Delta\Gamma} \tag{5}$$

allows one to obtain the distribution of activation energies for the mechanical and dielectric relaxations, shown in Figures 6 and 7, respectively. A low dispersion can be detected in the low-temperature zone of Figure 6, suggesting a distribution of activation entropies for the mechanical process. The average values for the activation enthalpies/entropies determined by means of the Eyring model amount to 14.0 kcal $mol^{-1}$/6.94 cal $mol^{-1}$ $K^{-1}$ and 10.5 kcal $mol^{-1}$ $K^{-1}$/1.83 cal $mol^{-1}$ $K^{-1}$ for the mechanical and dielectric $\beta$ processes. The relatively low values of the activation entropy suggest that the mechanical and dielectric $\beta$ processes can be considered simple relaxations in Starkweather terminology.[14]

A compliance function $\Gamma$ such as the mechanical compliance $D^*(\omega)$ or the dielectric permittivity $\epsilon^*(\omega)$ is related to decay function $\Phi(t)$ by[15]

$$\frac{\Gamma^*(\omega) - \Gamma_u}{\Gamma_r - \Gamma_u} = \int_0^\infty \left[-\frac{d\Phi(t)}{dt}\right] \exp(-i\omega t)\, dt \tag{6}$$

Since the complex modulus $M^*(\omega)$ is the reciprocal of the complex compliance ($M^*(\omega) = (\Gamma^*(\omega))^{-1}$), the electric and relaxation modulus can be written as

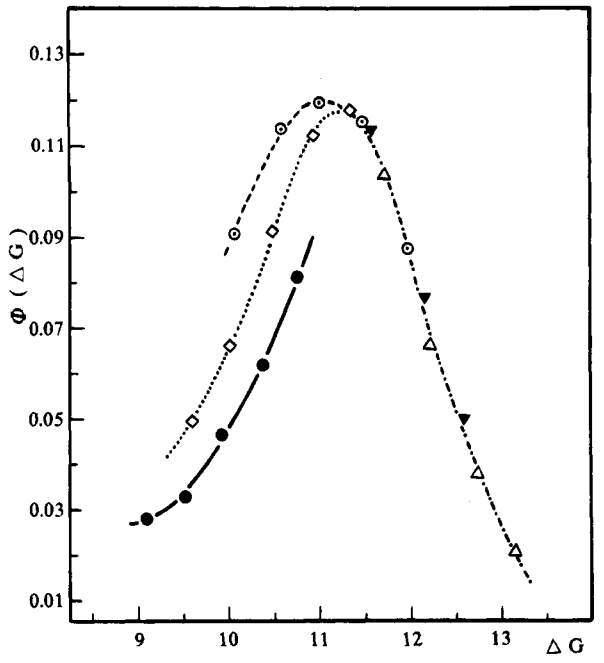


**Figure 6.** Distribution of free energies for the mechanical $\beta$ relaxation process.

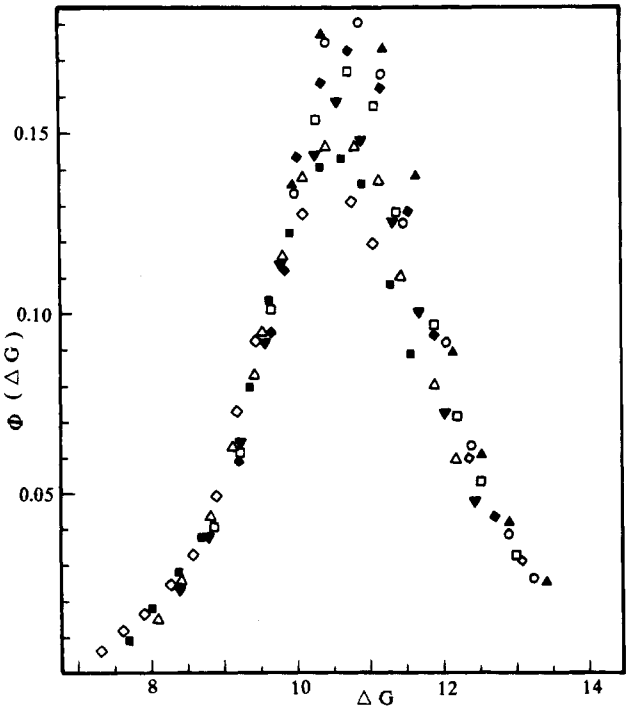


**Figure 7.** Distribution of free energies for the dielectric $\beta$ relaxation process.

$$\frac{M_u - M^*(\omega)}{M_u - M_r} = \int_0^\infty \left[-\frac{d\Phi(t)}{dt}\right] \exp(-i\omega t)\, dt \qquad (7)$$

Here as in eq 6 the subindices r and u refer to the relaxed and unrelaxed values of the compliance function, whereas the decay function, also called the Kohlrausch–Williams–Watts (KWW) function, is given by[16,17]

$$\Phi(t) = \exp\left[-\left(\frac{t}{\tau_0}\right)^{\bar{\gamma}}\right]; \quad 0 \le \bar{\gamma} \le 1 \qquad (8)$$

The exponent $\gamma$ depends on the distribution of relaxation times in the sense that its value is larger, the narrower the distribution is; for example, $\gamma = 1$ for a single relaxation time or Debye peak.

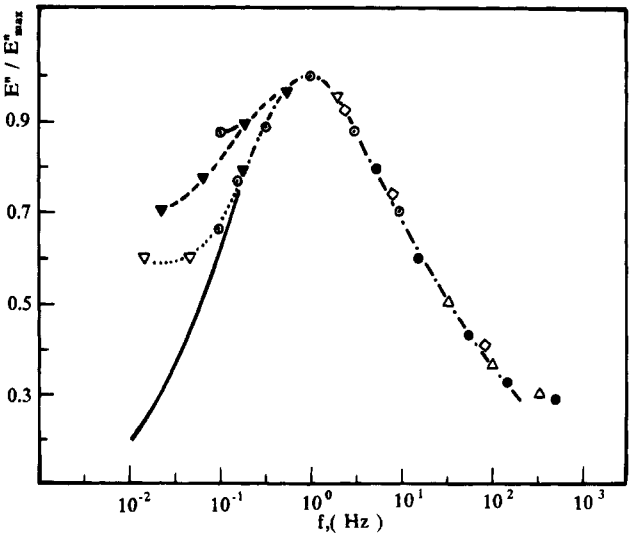


**Figure 8.** Normalized master curve for the mechanical $\beta$ relaxation process. The symbols represent results at the following temperatures: (▽) 137, (▼) −60, (⊙) −70, (◇) −80, (●) −90, and (△) −100 °C. The continuous line represents the Fuoss–Kirkwood curve which better fits the experimental results.

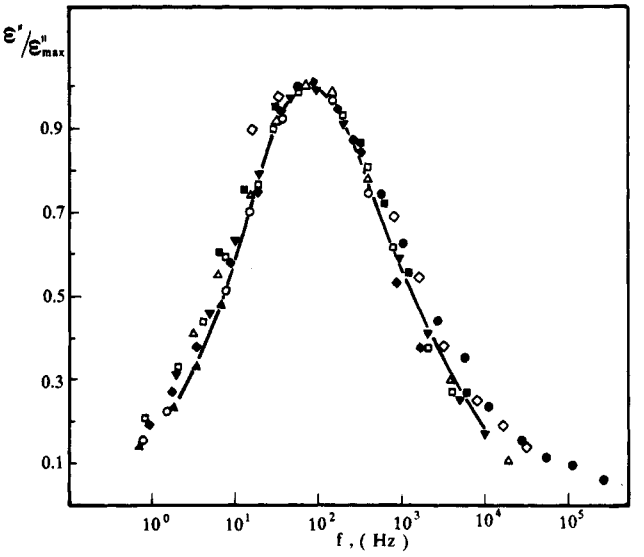


**Figure 9.** Normalized master curve for the dielectric $\beta$ relaxation process. The symbols represent results at the following temperatures: (▲) 0, (○) −10, (◆) −20, (□) −30, (▼) −40, (△) −50, (■), −60, (◇), −70, and (●) −80 °C.

Isotherms showing the frequency dependence of the normalized loss modulus in the $\beta$ region could be superposed by a simple translation along the log $\omega$ axis. The master curve for this process was obtained from the isotherms shown in Figure 4; the corresponding curve at −70 °C, represented in Figure 8, is fitted by using a KWW function with exponent 0.40 ± 0.02 in eq 7. The agreement between the calculated and experimental master curves is very good when the latter curves are drawn from the isotherms in which the contributions from the glass–rubber relaxation process were eliminated by using the procedure described before. The master curves for the dielectric $\beta$ relaxation process at −50 °C, represented in Figure 9, obey eq 6 by using $\gamma = 0.5$ for the exponent of the decay function. Here, as in the mechanical process, the contributions

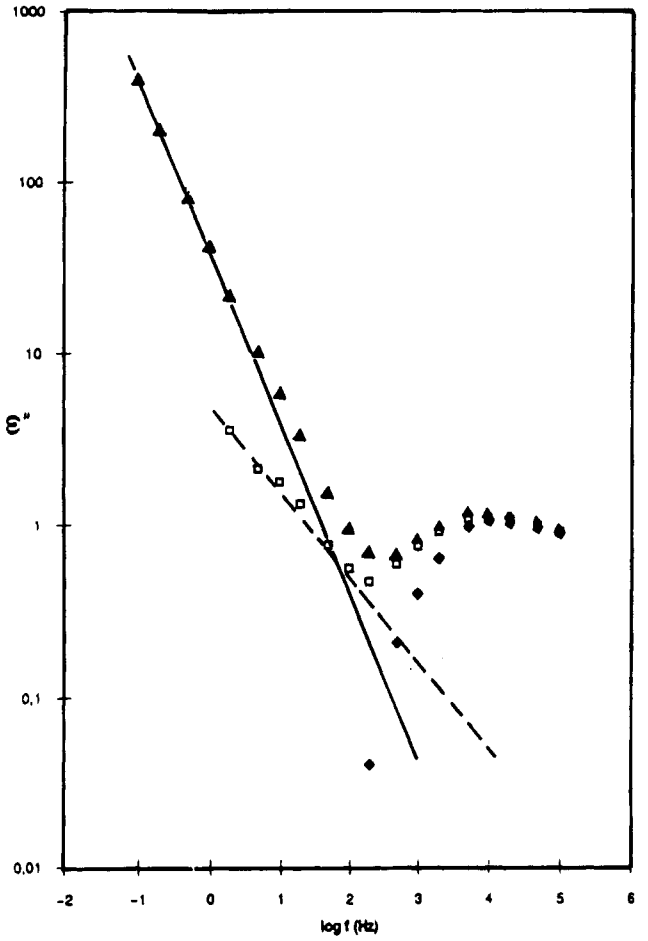


**Figure 10.** Frequency dependence of the dielectric loss on frequency. The symbols ▲, □, and ● represent respectively the total permittivity loss, the interfacial conductive loss, and the dipolar loss relaxation.

to the $\beta$ peaks from the $\alpha$ glass–rubber relaxation were taken off.

In order to compare the decay functions for the $\beta$ and $\alpha$ dielectric relaxations, the dielectric master curve was constructed by horizontal shifting of the corresponding isotherms. The evaluation of these isotherms for the dipolar $\alpha$ relaxation entails some difficulties due to the fact that conductive contributions become dominant at low frequencies, as can be seen in Figure 10 where the dielectric loss is represented as a function of frequency. Conductivity effects may arise from free charges and/or interfacial phenomena on the electrodes–polymer interface and, by assuming that additivity holds, the complex dielectric permittivity in the $\alpha$ relaxation process may be written as[18,19]

$$\epsilon^*(\omega) = \epsilon^*_d(\omega) + \epsilon^*_c(\omega) + \epsilon^*_i(\omega) \qquad (9)$$

where the subindices d, c, and i refer respectively to the dipolar, free charges, and interfacial contributions. The last two terms on the right-hand side of this equation can be expressed by

$$\epsilon^*_c(\omega) = \epsilon_{\infty c}[1 + (j\omega\tau_c)^{-1}]$$

$$\epsilon^*_i(\omega) = \epsilon_{\infty i}[1 + (j\omega\tau_i)^{-\bar{\alpha}}] \qquad (10)$$

where $\epsilon_{\infty c}$ and $\epsilon_{\infty i}$ represent respectively the free charges and the interfacial contributions at infinite frequency. According to this, the losses due to free charges $\epsilon''_c$ and

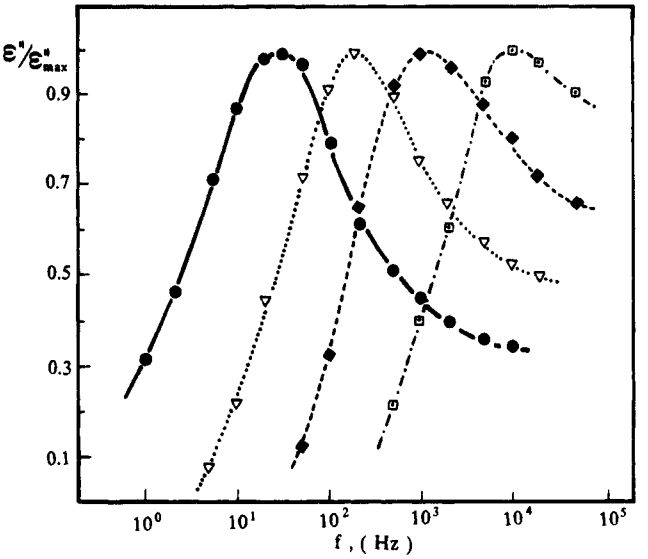


**Figure 11.** Normalized dielectric loss curves for the glass–rubber relaxation process at several temperatures: (●) 70, (▽) 80, (◆) 90, and (⊡) 100 °C.

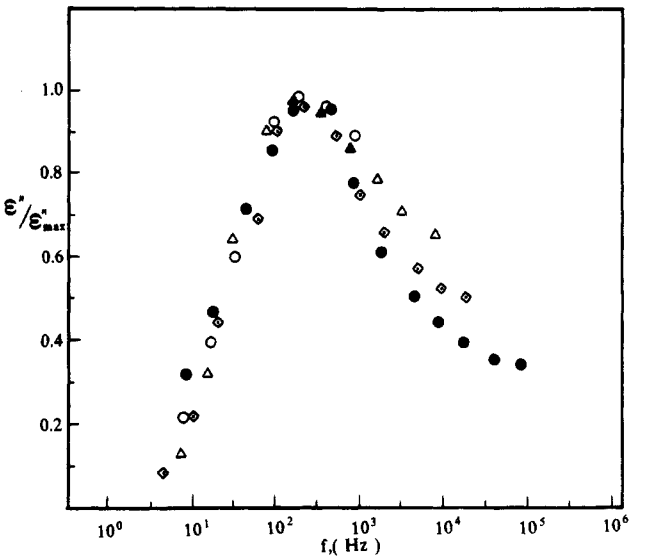


**Figure 12.** Normalized master curve for the dielectric glass–rubber relaxation. The symbols represent results at the following temperatures: (●) 70, (◇) 80, (▲) 90, and (○) 100 °C.

to interfacial phenomena $\epsilon''_i$ scale with frequency as

$$\epsilon''_c(\omega) \sim \omega^{-1}$$

$$\epsilon''_i(\omega) \sim \omega^{-\bar{\alpha}} \qquad (11)$$

where $\alpha$ is ca. 0.5. The dipolar loss $\epsilon''_d$ was determined by subtracting from the experimental results, $\epsilon''(\omega)$, the conductivity loss due to free charges and to interfacial phenomena using the scaling relations given above, and the results obtained are shown in Figure 11. The master curve obtained for the glass–rubber relaxation process from these isotherms is shown in Figure 12, where it can be seen that overlapping of the dielectric glass–rubber relaxation with the $\beta$ process gives rise to a bad superposition of the isotherms in the high-frequency zone, and, as a consequence, the value of the exponent for the KWW expression (=0.40–0.56) is somewhat uncertain.

The normalized mechanical curves corresponding to the mechanical $\alpha$ relaxation are respresented as a

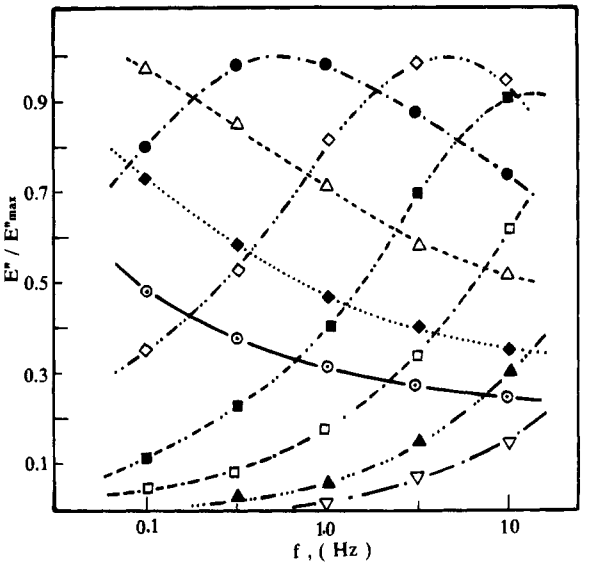


**Figure 13.** Frequency dependence of the normalized loss relaxation modulus at several temperatures: (⊙) 35, (◆), 40, (△) 45, (●) 50, (◇) 55, (■) 60, (□) 65, (▲) 70, and (▽) 75 °C.

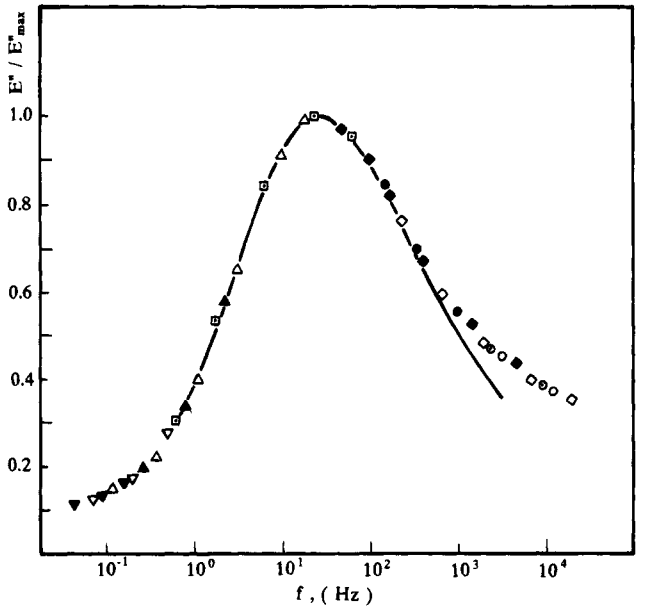


**Figure 14.** Normalized master curve for the mechanical glass–rubber relaxation. The symbols represent results corresponding to the following temperatures: (⊙) 30, (○) 35, (◇) 40, (◆) 45, (●) 50, (⊡) 55, (△) 60, (▲) 65, (▽) 70, and (▼) 75 °C.

function of frequency in Figure 13. By horizontal shifting of the isotherms, the master curve shown in Figure 14 is obtained. The frequency dependence of the normalized master curve is fitted by eq 7 for $\gamma = 0.36$.

## Discussion

An important issue in the analysis of the dynamics of polymers is to elucidate the molecular motions from which subglass relaxations arise. In the case of PCCHA, dipolar activity arising from equatorial $\rightleftarrows$ axial changes of the chlorine atom in the cyclohexyl group, as a consequence of chair-to-chair conformational transitions in the cyclohexane ring, was held mainly responsible for the dielectric $\beta$ subglass relaxation.[8] As can be seen in Figure 15, the dipole moment of the side group is the result of the combination of the dipole moment of 1.775 D associated with the ester group whose orientation forms an angle of 123° with the

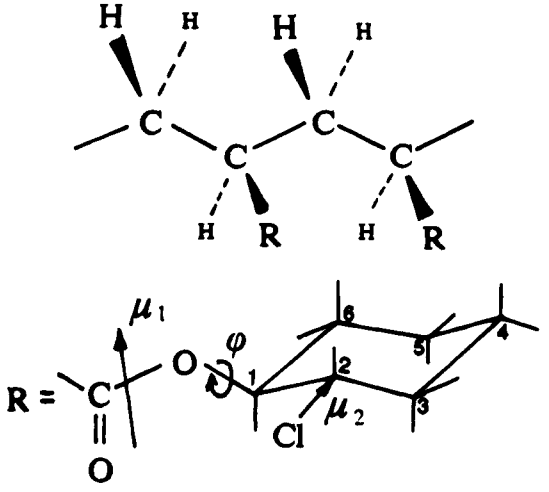


**Figure 15.** Scheme of a meso diad in the trans configuration. The arrows in the side groups represent the direction of the polar groups.

C–CO bond[20] and the dipole moment of 1.9 D corresponding to the C–Cl bond.[21] Changes in the relative positions of the dipole moments associated with the ester and the C–Cl bonds could produce the subglass relaxation. In order to check this possibility, the NMR spectra of the polymer were critically interpreted, as will be shown below.

The $^1$H NMR spectrum of the polymer presents eight signals in the interval $\delta$ 3.786–3.865 corresponding to the hydrogen bound to the $C_2$ atom in the cyclohexyl group, these signals appearing in the interval $\delta$ 4.729–4.806 for the hydrogen bound to the $C_1$ atom. This arrangement permits one to conclude that the hydrogen atoms bound to the $C_1$ and $C_2$ atoms are in axial positions in the cyclohexyl group in the chair conformation, and, therefore, the halogen and oxygen atoms are equatorial. This conclusion is also supported by the values of the H,H vicinal coupling constants between the hydrogens of the $C_1$, $C_2$, and $C_3$ carbons and between those of the $C_1$, $C_2$, and $C_6$ carbons; for example, the $^1$H NMR spectrum presents coupling constants of $J(H_{2a},H_{1a})$ = 9.0 Hz, $J(H_{2a},H_{3a})$ = 10.4 Hz, and $J(H_{2a},H_{3c})$ = 4.2 Hz for the hydrogen at $C_2$ and $J(H_{1a},H_{2a})$ = 9.2 Hz, $J(H_{1a},H_{3a})$ = 9.4 Hz, and $J(H_{1a},H_{6a})$ = 4.6 Hz for the hydrogen at $C_1$. This spectrum can only be justified by assuming a chair conformation with equatorial positions of the oxygen and chlorine atoms. This analysis rules out the presence of the heteroatoms in axial positions, and, as a consequence, chair-to-chair conformational transitions in the cyclohexyl group do not seem to be the origin of the $\beta$ subglass process exhibited by the dielectric spectrum.

The curves that describe the changes in energy arising from rotations about the O–$C_y$ bonds in the side groups indicate that the minima of energy are located at $\phi = 0°$ and 180° at which the dipole moments are 2.90 and 1.78 D, respectively, the energy associated with the latter rotational state being nearly 2 kcal mol$^{-1}$ above that of the alternative one.[19] Conformational studies reported elsewhere[19] for 2-chlorocyclohexyl acrylate (CCHI) and PCCHA indicate that the rotational angle $\phi = 0°$ and the equatorial linkage of the Cl atom to the cyclohexyl group gives a good account of the equilibrium dielectric properties of these systems. Therefore, it is possible that the $\beta$ relaxation may come only from conformational transitions $\chi = 0 \leftrightarrows \chi = \pi$ about the C–CO bonds of the side groups and hence the

relaxation strength of the $\beta$ process for PCCHA is relatively weak, only 0.35 at −70 °C, in spite of the apparent conformational versatility of the side group. In fact this strength is only ca. 30% larger than that of the $\beta$ relaxation process for poly(cyclohexyl acrylate) (PCHA).[22] It should be pointed out that conformational changes about O−C$^{ar}$ bonds in poly(2-chlorophenyl acrylate) are mainly responsible for the prominent $\beta$ absorption exhibited by this polymer whose strength is comparable to that of the α glass−rubber relaxation process.[23,24]

Whereas modeling of mechanical subglass processes involves serious difficulties, dielectric relaxations are amenable to evaluation by the statistical mechanics procedure. Recently Boyd and co-workers[4] developed a method that renders feasible the evaluation of the relaxation strength of dielectric subglass processes. The method is based on the assumption that subglass relaxations are caused by intramolecular conformational transitions occurring in the flexible side groups. The theory predicts that the intramolecular correlation coefficient of the relaxing dipoles in the glassy state can be written as[4]

$$g_\beta = \frac{1}{x\mu_0^2}[\langle m^2\rangle - \langle \mathbf{m}\rangle\cdot\langle \mathbf{m}\rangle] \tag{12}$$

where $x$ is the degree of polymerization and $m = \Sigma\mu_i(\chi)$ is the dipole moment associated with the conformation $\chi$. By assuming that $\langle \mu_i\cdot\mu_j\rangle \approx \langle \mu_i\rangle\cdot\langle \mu_j\rangle$, eq 12 becomes

$$g_\beta = \frac{1}{x\mu_0^2}[\sum_k \mu_k^2 - \sum_k (p_k(1)^2 + p_k(2)^2)\mu_k^2 + 2p_k(1)\,p_k(2)\,\boldsymbol{\mu}_k(1)\cdot\boldsymbol{\mu}_k(2)] \tag{13}$$

where $p_k(1)$ and $p_k(2) = 1 - p_k(1)$ represent the probability of occurrence of the states $\chi = 0$ and $\chi = \pi$ about the C−CO bond, these states being respectively those in which the carbonyl group is cis and trans to the methine bond. Conformational calculations reported elsewhere indicate that the state $\chi = \pi$ has an energy of ca. 0.6 kcal mol$^{-1}$ below that of the alternative conformational state.[23] It is expected that as the temperature decreases in the glassy state the conformational population associated with the state $\chi = \pi$ will increase.

The dipolar correlation coefficient $g_\beta$ can be experimentally determined by means of Onsager[25] type equations such as the Fröhlich relation[26]

$$g_\beta = \frac{9(2\epsilon_{r\beta} + \epsilon_{\mu\beta})(\epsilon_{r\beta} - \epsilon_{\mu\beta})}{\epsilon_{r\beta}(\epsilon_{\mu\beta} + 2)^2\mu_0^2}\frac{M_0 k_B T}{4\pi\varrho N_A} \tag{14}$$

where $M_0$ is the molecular weight of the repeating unit, $T$ is the absolute temperature, $k_B$ and $N_A$ are respectively the Boltzmann constant and Avogadro's number, $\varrho$ is the density of the polymer, and $\mu_0$ (=2.90 D) is the modulus of the dipole moment associated with the repeating unit. Complex dielectric plots of the experimental results in the $\beta$ region give $\epsilon_{r\beta} = 2.65$ and $\epsilon_{\mu\beta} = 2.30$ at −70 °C, and by substituting these values in eq 14, one obtains that $g_\beta \approx 0.04$. The low value of $g_\beta$ suggests a strong correlation between dipoles; that is, conformational changes in very few side groups may produce the dipolar absorption at the temperature indicated. The fraction of groups involved in the development of the $\beta$ process was obtained by means of eq 13 for different values of $p_k(2)$. Thus by assuming $p_k(2) = 0.73$, $g_\beta = 0.24$, which is significantly higher than the value of this quantity determined from the experimental results; this value decreases to 0.06 for $p_k(2) = 0.95$. As occurs in PCHA,[22] conformational transitions in about 6% of the C−CO bonds will nearly produce the dielectric activity found for PCCHA at −70 °C. As the temperature increases the relaxation strength increases and, according to eq 13, the dipolar correlation coefficient will be an increasing function of temperature. Therefore, the groups involved in the $\beta$ process will increase as the temperature goes up.

The mechanical relaxation spectrum of PCCHA presents a $\beta$ subglass relaxation which in polymers with cyclohexyl groups in their structure was traditionally attributed to flipping of this group from a chair conformation to another.[5,8] This motion, however, may not be held responsible for the $\beta$ absorption in PCCHA in view of the NMR spectrum of the polymer which indicates that the oxygen and halogen atoms are both linked in equatorial positions to the cyclohexane ring. The low-temperature relaxation may entail motions in the side groups alone or coupled with conformational transitions in the main chain which do not produce a significant displacement in the chain tails. It should be pointed out that a quantitative molecular theory that predicts the relaxation magnitude has not been developed yet.

Close to the glass transition temperature, amorphous polymers and, in general, glass-forming liquids display temperature dependences of relaxation times which differ from that exhibited by single activated processes. For thermorheologically simple systems, the average relaxation time $\tau$ shows a temperature dependence that is given by the empirical Vogel−Fulcher−Tammann−Hesse equation[27]

$$\ln \tau_i = A + \frac{m}{T - T_\infty} \tag{15}$$

The relaxation time is also related to the relative free volume $\varphi$ as indicated by the empirical Doolittle expression[28]

$$\tau = A' \exp(\beta/\varphi) \tag{16}$$

where $B$ is an empirical parameter close to 1 and $A'$ is a constant. By assuming that the volume is a linear function of temperature, eq 16 leads to eq 15 and, as a consequence, $T_\infty$ in this relation can be viewed as the temperature at which the free volume would be zero were it not for the formation of the glassy state. Semilogarithmic plots showing the dependence of the relaxation times on $(T - T_\infty)^{-1}$ are shown in Figure 16 for the mechanical and dielectric relaxations, respectively. The fraction of relative free volume can be obtained from the slopes $m$ of the straight lines of these figures by means of the relation

$$\frac{\varphi_g}{B} = \frac{T_g - T_\infty}{m} \tag{17}$$

that can easily be obtained by comparing the Doolittle and the VTH equations. The values obtained for these quantities from the dielectric and mechanical experimental results amount to 0.038 and 0.042, respectively. These results, similar to those obtained for PCHA, are significantly larger than the average value of 0.025 ± 0.05 reported for most systems. If the iso-free-volume theory at $T_g$ holds, the relatively high values of $\varphi_g/B$ could be explained in terms of the Cohen−Turnbull free

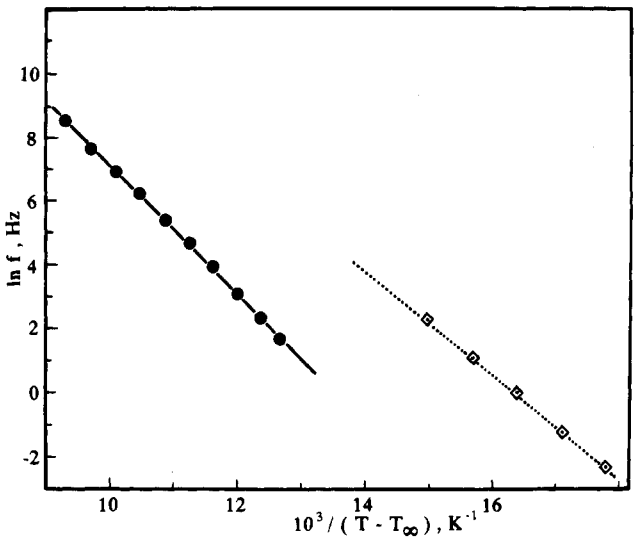


**Figure 16.** Doolittle plot for the mechanical (◇) and dielectric (●) glass–rubber relaxations.

volume theory, according to which[29]

$$B = \gamma v^*/v_m \tag{18}$$

where $\gamma$ is an empirical parameter ($\approx$0.5) and $v^*$ and $v_m$ are respectively the critical volume necessary for a relaxation process to take place and the volume of the segments involved in the process. Since $B < 1$, the theory suggests that $v_m > v^*$.

The exponent $\gamma$ in the KWW equation, which has traditionally been interpreted in terms of the distribution of relaxation times, has recently been explained by means of the coupling scheme which views the relaxation as a combination of a primary relaxation mechanism, caused by interaction of the relaxing species with the heat bath, and another coupling mechanism involving interactions between the relaxing species, which provide a nonnegligible time-dependent effect on the primary relaxation process already in progress. Thus the decay function $\Phi(t)$ reflects the slow down of the primitive rate by time-dependent constraints coming from the interactions between the relaxing species. The theory[30,31] predicts two coupled relations: a KWW form for the relaxation function

$$\varphi(t) \approx \exp[-(t/\tau^*)^{1-n}] \tag{19}$$

and a relation between the effective relaxation time $\tau^*$ and the relaxation time associated with the primary relaxation mechanism, $\tau_o$, given by

$$\tau^* = [(1 - n)\omega_c{}^n\tau_o]^{1/(1-n)} \tag{20}$$

where $\omega_c{}^{-1}$ is a time characteristic depending on the interactions between the relaxing species and $n(=1 - \gamma)$ in the two last equations is a parameter characterizing the coupling between the relaxing species. The fact that the value of $n$ is 0.64 and 0.5 for the mechanical and dielectric glass–rubber relaxation suggests, according to this scheme, more complicated coupled mechanisms involved in the former relaxation than in the latter.

The $\beta$ relaxation is believed to involve a weighted sum of elementary processes occurring in a variety of local environments, and, as a consequence, it is in most cases a rather broad process in the frequency domain. The $\alpha$ relaxation occurs after collapsing the local environment and compared to the $\beta$ process is for most systems a narrow process in the frequency domain.[32] It is therefore surprising that the exponent of the decay function for the dielectric $\beta$ processes is similar to that exhibited by the $\alpha$ glass–rubber relaxations, and in the case of the $\beta$ mechanical relaxation the exponent is even slightly higher than that corresponding to the glass–rubber relaxation. This behavior can only be explained by assuming that very limited local processes produce the subglass absorptions.

**Acknowledgment.** This work was supported by the DGCYT through the Grant PB-92-0773.

## References and Notes

(1) Heijboer, J. *Ann. N.Y. Acad. Sci.* **1976**, *279*, 105.
(2) Boyd, R. H. *Polymer* **1985**, *26*, 323.
(3) Buerger, D.; Boyd, R. H. *Macromolecules* **1989**, *22*, 2694 and 2699.
(4) Smith, G. D.; Boyd, R. H. *Macromolecules* **1991**, *24*, 2731.
(5) Heijboer, J. Doctoral Thesis, Leiden University, Leiden, The Netherlands, 1972.
(6) Díaz-Calleja, R.; Ribes, A.; Gómez, J. L.; Riande, E.; Guzmán, J. *Macromolecules* **1988**, *21*, 2121.
(7) Díaz-Calleja, R.; Ribes, A.; Gómez, J. L.; Riande, E.; Guzmán, J. *Macromolecules* **1989**, *22*, 1821.
(8) McCrum, N. G.; Read, B. E.; Williams, G. *Anelastic and Dielectric Effects on Polymeric Solids*; Wiley-Interscience: New York, 1967.
(9) Díaz-Calleja, R.; Riande, E.; San Román, J. *J. Polym. Sci., Part B: Polym. Phys.* **1992**, *30*, 1239.
(10) Fuoss, R.; Kirkwood, J. G. *J. Am. Chem. Soc.* **1941**, *63*, 385.
(11) Reference 8, p 118.
(12) Reference 8, p 115.
(13) Tschoegl, N. W. *The Phenomenological Theory of Linear Viscoelastic Behavior*; Springer-Verlag: Berlin, Heidelberg, 1989, p 201.
(14) Starkweather, H. W. *Macromolecules* **1981**, *14*, 1277; **1990**, *23*, 328.
(15) Williams, G.; Watts, D. C.; Dev, S. B.; North, A. M. *Trans Faraday Soc.* **1971**, *67*, 1223.
(16) Kohlrausch, R. *Ann. Phys.* **1847**, *12* (3), 3931.
(17) Williams, G.; Watts, D. C. *Trans. Faraday Soc.* **1970**, *66*, 80.
(18) Díaz-Calleja, R.; Riande, E.; San Román, J. *J. Phys. Chem.* **1993**, *97*, 4848.
(19) Díaz-Calleja, R.; Riande, E.; San Román, J.; Compañ, V. *Macromolecules* **1994**, *27*, 2092.
(20) Saiz, E.; Hummel, J. P.; Flory, P. J.; Plavsic, M. *J. Phys. Chem.* **1981**, 485, 3211.
(21) McClellan, A. L. *Table of Experimental Dipole Moments*; Rahara: El Cerrito, CA, 1974; Vol. II.
(22) Díaz-Calleja, R.; Riande, E.; San Román, J. *Macromolecules* **1992**, *25*, 2875.
(23) Díaz-Calleja, R.; Riande, E.; San Román, J. *Macromolecules* **1991**, *24*, 264. *J. Phys. Chem.* **1992**, *96*, 931.
(24) Díaz-Calleja, R.; Riande, E.; San Román, J. *J. Non-Crystalline Solids* **1991**, *131–133*, 852.
(25) Onsager, L. *J. Am. Chem. Soc.* **1936**, *58*, 1486.
(26) Fröhlich, H. *Theory of Dielectrics*, 2nd ed.; Oxford University Press: Oxford, U.K., 1959.
(27) Vogel, K. *Phys. Z.* **1921**, *22*, 645.
(28) Doolittle, A. K.; Doolittle, D. B. *J. Appl. Phys.* **1957**, *28*, 901.
(29) Cohen, M. H.; Turnbull, D. J. *J. Chem. Phys.* **1954**, *31*, 1164.
(30) Ngai, K. L.; Rajagopal, A. K.; Teitler, A. K. *J. Chem. Phys.* **1988**, *88*, 5086.
(31) Ngai, K. L.; Mashimo, S.; Fytas, G. *Macromolecules* **1988**, *21*, 3030.
(32) Williams, G. *Adv. Polym. Sci.* **1979**, *33*, 59.

MA9410577